Research Square

Preprints are preliminary reports that have not undergone peer review.
They should not be considered conclusive, used to inform clinical practice,
or referenced by the media as validated information.

Robust fractional-order fixed-time terminal sliding mode control for robot manipulators

Chuong Vo Lam
Ho Chi Minh City University of Technology and Engineering
Ngoc Thanh Ha Le Nhu
Ho Chi Minh City University of Technology and Engineering
Luan Vu Truong Nguyen
vuluantn@hcmute.edu.vn

Ho Chi Minh City University of Technology and Engineering

Article

Keywords: Fast terminal sliding surface, Fractional-order sliding suface, Lyapunov stability, Finite time convergence, Robot manipulators

Posted Date: March 9th, 2026

DOI: https://doi.org/10.21203/rs.3.rs-8932994/v1

License: This work is licensed under a Creative Commons Attribution 4.0 International License.
Read Full License

Additional Declarations: No competing interests reported.

Robust fractional-order fixed-time terminal sliding mode control for robot manipulators

Vo Lam Chuong[1], Ha Le Nhu Ngoc Thanh[1], and Truong Nguyen Luan Vu[2*]
[1]Mechatronics Department, Ho Chi Minh City University of Technology and Engineering, Viet Nam
[2]Mechanical Faculty, Ho Chi Minh City University of Technology and Engineering, Viet Nam
[*]Corresponding author, email: vuluantn@hcmute.edu.vn

Abstract. This paper addresses the robust trajectory tracking problem for robotic manipulators in the presence of parametric uncertainties and external disturbances. A novel fractional-order sliding manifold is constructed to guarantee fixed-time convergence independent of initial conditions. The proposed control strategy combines fractional-order calculus with fixed-time terminal sliding mode control, thereby ensuring global finite-time stability while significantly enhancing robustness against modeling uncertainties and perturbations. The stability analysis based on Lyapunov theory confirms fixed-time convergence of the closed-loop system. To alleviate chattering and improve control smoothness, the discontinuous signum function in the control law is replaced by a continuously differentiable nonlinear function, leading to optimized gain adaptation and reduced control oscillations. The proposed method achieves superior tracking accuracy, faster convergence, and substantial chattering attenuation compared with existing approaches. Comprehensive numerical simulations and comparative studies validate the effectiveness and robustness of the proposed controller.

Keywords. Fast terminal sliding surface, Fractional-order sliding suface, Lyapunov stability, Finite time convergence, Robot manipulators.

1. Introduction

Robot manipulators play an essential role in a wide range of modern applications, including industrial automation, space missions, and medical interventions, where high precision trajectory tracking is crucial. However, achieving accurate control performance remains challenging due to the inherent nonlinear dynamics of manipulators, strong coupling effects, as well as the presence of various uncertainties caused by model mismatches, payload variations, and external disturbances, and so on. To overcome these issues, advanced control methods like feedback linearization control [1–2], model predictive control [3], adaptive control [4], robust control [5], fuzzy and neural network control [6–7] and sliding mode control (SMC) [8–10] have been extensive researched.

Among these techniques, SMC has been widely adopted because of its structural simplicity, fast transient response, and strong robustness. However, conventional SMC addresses linear sliding surfaces, which only ensure the asymptotic convergence of system states, and to achieve the faster

convergence, it normally results in high control gains, which lead to saturation zones of actuators, induce the well-known chattering phenomenon, and excite unmodelled high-frequency dynamics. To overcome these limitations, terminal sliding mode control (TSMC) was introduced to obtain finite-time convergence without the cost of large control efforts [11–12]. The main disadvantage of the TSMC methods is the singularity problem, which deteriorates the system performance in terms of tracking control and system stability. Therefore, a nonsingular terminal sliding mode control (NTSMC) [12–16] was proposed to eliminate the singularity by choosing appropriate fractional power terms in control laws. Nonsingular fast TSM control (NFTSMC) was proposed in [17–20] to increase the speed of convergence while maintaining typical specifications of NTSMC such as singularity avoidance and chattering reduction. Therefore, the NFTSMC becomes increasingly popular for high-speed and precision tracking control of robot manipulators.

Fractional calculus has a long history in the mathematical field, but it has only been developed in recent decades in the control field since Podlubny proposed a fractional-order proportional integral derivative (PID) controller [21]. Fractional-order (FO) controllers extend classical differentiation and integration to non-integer orders, which give some advantages such as additional flexibility, improved transient performance, and enhanced robustness [22–25]. The main disadvantage of the FO controller is the computation burden, but thanks to the rapid development of microprocessors to help solve the problem of computing capabilities.

Recent studies have demonstrated the advantages of combining fractional-order design with terminal SMC to achieve better performance of controllers in terms of fast convergence, less control efforts, and chattering-free. Fractional-order terminal sliding mode controllers (FOTSMC) [26–27] were first suggested to handle these problems. The controller ensured the finite-time convergence and high trajectory tracking performance, but still had chattering in control inputs. Based on these controllers, other authors have recently introduced the fractional-order non-singular terminal sliding mode controllers (FONTSMC) [25], [28–30] to eliminate singularity in the control law and also obtain a better performance in tracking control problem under the presence of uncertainties and external disturbances. Although these controllers provide finite-time tracking error convergence and effectively handle the issue of unbounded control inputs, they still suffer from chattering and large control efforts.

The purpose of this work is to propose an efficient control method for tracking control of robot manipulators that meet those strict requirements. The advantageous characteristics of the fractional derivative are that it utilizes the memory of previous values and has a large stability region, with more parameters to tune, which helps enhance the system performance. Hence, this study proposes to incorporate the fractional derivative into the sliding surface and control law to achieve faster convergence, finite-time stability of the closed-loop system, and the control efforts within an appropriate range, while maintaining chattering-free control signals.

This paper is organized as follows. Section 2 briefly introduces the fractional calculus, some properties and related theorems are mentioned. The dynamic model for n- degree-of-freedom (*n*-dof) robot manipulators is also provided in this section. In Section 3, the proposed method is presented, and the stability of the closed-loop system is also proved. Section 4 is a simulation study. Finally, conclusions are given in Section 5.

2. Preliminaries

2.1. Fractional calculus

Fractional calculus introduces a general form of integral and derivative computation. The fractional differ-integration is given in the following form:

$$ {}_{a}D_{t}^{\alpha} = \begin{cases} \dfrac{d^{\alpha}}{dt^{\alpha}} & (\alpha > 0) \\ 1 & (\alpha = 0) \\ \displaystyle\int_{a}^{t} (dt)^{-\alpha} & (\alpha < 0) \end{cases} \tag{1} $$

where ${}_{a}D_{t}^{\alpha}$ is the fractional-order integrodifferential operator with the order $\alpha \in \mathbb{R}$. The limitations of the operator are defined by *a* and *t*.

The three well-known definitions of FO derivatives are most commonly used in the control field: Riemann-Liouville (RL), Grünwald–Letnikov (GL), and Caputo. The last one is more common in engineering applications, since this definition integrates initial conditions that have a practical physical meaning in traditional way.

*Definition 1***.** The Caputo fractional derivative of order $\alpha > 0$ of a function *f*(*t*) is given by [22]

$$ {}_{a}D_{t}^{\alpha} f(t) = \frac{1}{\Gamma(n-\alpha)} \int_{a}^{t} \frac{f^{(n)}(\tau)}{(t-\tau)^{\alpha-n+1}} d\tau, \quad (t > a) \tag{2} $$

with $n = \min\{k \in \mathbb{R} \,/\, k > \alpha\}$; $\Gamma(.)$ is the Gamma function.

*Definition 2***.** The Grünwald–Letnikov fractional derivative of α^{th}-order of a function *f*(*t*) is defined as follows

$$ {}_{a}D_{t}^{\alpha} f(t) = \lim_{h \to 0} h^{-\alpha} \sum_{j=0}^{[(t-a)/h]} (-1)^{j} \binom{\alpha}{j} f(t - jh) \tag{3} $$

where *h* is a step time; [.] represents an integer part; $\binom{\alpha}{j} = \dfrac{\alpha(\alpha-1)...(\alpha-j+1)}{j!}$

Equation (3) is used to obtain the numerical solution for the fractional-order differential equation.

Property 1. If the fractional derivative ${}_aD_t^{\alpha} f(t)$ of a function $f(t)$ is integrable

$$ {}_aI_t^{\alpha}\left({}_aD_t^{\alpha} f(t)\right) = f(t) - \sum_{j=1}^{k}\left[{}_aD_t^{\alpha-j} f(t)\right]_{t=a} \frac{(t-a)^{\alpha-j}}{\Gamma(\alpha-j+1)} \tag{4} $$

Property 2. For fractional orders $\alpha, \beta > 0$, the following equalities are valid for the fractional derivative and integral operation (Podlubny 1988):

$$ \begin{aligned} &D^{\alpha}\left(D^{\beta} f(t)\right) = D^{\alpha+\beta} f(t) \\ &D^{\alpha}\left(D^{-\beta} f(t)\right) = D^{\alpha-\beta} f(t) \\ &D^{\alpha}\left(D^{-\alpha} f(t)\right) = D^{\alpha-\alpha} f(t) = f(t) \end{aligned} \tag{5} $$

Theorem 1. Let $x = 0$ be an equilibrium point for the non-autonomous fractional-order system: $D^{\alpha} x(t) = f(x,t)$ where $f(x,t)$ satisfies the Lipschitz condition with Lipschitz constant $l > 0$. Assume that there exist a Lyapunov function $V(t, x(t))$ satisfying:

$$ \alpha_1 \|x\|^{a} \le V(x,t) \le \alpha_2 \|x\| \tag{6} $$

$$ \dot{V}(x,t) \le \alpha_3 \|x\| \tag{7} $$

where $\alpha_1, \alpha_2, \alpha_3$ and a are positive constants. Then the equilirium point of the system is Mittag-Leffler stable.

Remark 1. Mittag-Leffler stability implies asymptotical stability [31]

Theorem 2. Let $x = 0$ be an equilibrium point for the non-autonomous fractional-order system: $D^{\alpha} x(t) = f(x,t)$

Assume that there exist a Lyapunov function $V(t, x(t))$ and class-K function $\alpha_i,\ i = 1,2,3$ satisfying:

$$ \alpha_1 \|x\| \le V(x,t) \le \alpha_2 \|x\| \tag{8} $$

$$ D^{\beta} V(x,t) \le -\alpha_3 \|x\|, \qquad \beta \in (0,1) \tag{9} $$

Then the equilirium point of system is asymptotically stable.

Lemma 1. Assume that a continuous positive definite function $V(t)$ satisfies the differential inequality

$$ \dot{V}(x,t) \le -\alpha V^{\beta}(t), \quad \forall t \ge t_0, \quad V(t_0) \ge 0 \tag{10} $$

where $\alpha > 0,\ 0 < \beta < 1$ are constants. Then, for any given $t_0, V(t)$ satisfies the inequality

$$ V^{1-\beta}(t) \le V^{1-\beta}(t_0) - \alpha(1-\beta)(t-t_0), \ \ t_0 \le t \le t_1 \tag{11} $$

and $V(t)=0,\ \ \forall t \geq t_1$, with t_1 given by:

$$t_1 = t_0 + \frac{V^{1-\beta}(t_0)}{\alpha(1-\beta)} \tag{12}$$

2.2. Dynamics of robot manipulators

Consider *n*-joints robot manipulators, its dynamic equation can be expressed as follows:

$$\boldsymbol{M}(\boldsymbol{q})\ddot{\boldsymbol{q}} + \boldsymbol{C}(\boldsymbol{q},\dot{\boldsymbol{q}}) + \boldsymbol{G}(\boldsymbol{q}) = \boldsymbol{\tau} + \boldsymbol{\tau}_d \tag{13}$$

Where $\boldsymbol{q},\ \dot{\boldsymbol{q}},\ \ddot{\boldsymbol{q}} \in \mathbb{R}^{1\times n}$ represents the vectors of joint position, velocity, and acceleration, respectively; $\boldsymbol{M}(\boldsymbol{q}) \in \mathbb{R}^{n\times n}$, $\boldsymbol{C}(\boldsymbol{q},\dot{\boldsymbol{q}}) \in \mathbb{R}^{n\times n}$, and $\boldsymbol{G}(\boldsymbol{q}) \in \mathbb{R}^{1\times n}$ stand for the symmetric positive definite inertia matrix, the centrifugal-Coriolis matrix, and the gravitational torque, respectively; $\boldsymbol{\tau}$ and $\boldsymbol{\tau}_d$ are the control torque input vector, and the external disturbance vector, respectively.

Assumption 1. The robot manipulator (13) has uncertainties in its dynamic equation:

$$\begin{aligned}
\boldsymbol{M}(\boldsymbol{q}) &= \boldsymbol{M}_0(\boldsymbol{q}) + \Delta\boldsymbol{M}(\boldsymbol{q}) \\
\boldsymbol{C}(\boldsymbol{q},\dot{\boldsymbol{q}}) &= \boldsymbol{C}_0(\boldsymbol{q},\dot{\boldsymbol{q}}) + \Delta\boldsymbol{C}(\boldsymbol{q},\dot{\boldsymbol{q}}) \\
\boldsymbol{G}(\boldsymbol{q}) &= \boldsymbol{G}_0(\boldsymbol{q}) + \Delta\boldsymbol{G}(\boldsymbol{q})
\end{aligned} \tag{14}$$

where $\boldsymbol{M}_0(\boldsymbol{q}),\ \boldsymbol{C}_0(\boldsymbol{q},\dot{\boldsymbol{q}}),$ and $\boldsymbol{G}_0(\boldsymbol{q})$ are the nominal parts of robot manipulators (estimated terms), whereas $\Delta\boldsymbol{M}(\boldsymbol{q}),\ \Delta\boldsymbol{C}(\boldsymbol{q},\dot{\boldsymbol{q}}),$ and $\Delta\boldsymbol{G}(\boldsymbol{q})$ represent the uncertainties terms.

Assumption 2. The dynamic equation of the robot manipulator (13) can be re-written as follows:

$$\boldsymbol{M}_0(\boldsymbol{q})\ddot{\boldsymbol{q}} + \boldsymbol{C}_0(\boldsymbol{q},\dot{\boldsymbol{q}}) + \boldsymbol{G}_0(\boldsymbol{q}) = \boldsymbol{\tau} + \boldsymbol{F}_d(\boldsymbol{q},\dot{\boldsymbol{q}},\ddot{\boldsymbol{q}}) \tag{15}$$

where $\boldsymbol{F}_d(\boldsymbol{q},\dot{\boldsymbol{q}},\ddot{\boldsymbol{q}}) = \boldsymbol{\tau}_d - \Delta\boldsymbol{M}(\boldsymbol{q})\ddot{\boldsymbol{q}} - \Delta\boldsymbol{C}(\boldsymbol{q},\dot{\boldsymbol{q}}) - \Delta\boldsymbol{G}(\boldsymbol{q}) \in \mathbb{R}^{n\times n}$ is the lumped disturbances, which includes the external disturbance and the system uncertainties.

Similar to some literature [32–33], $\boldsymbol{M}_0(\boldsymbol{q})$ is chosen as

$$\boldsymbol{M}_0 = \frac{2}{\underline{m} + \bar{m}}\boldsymbol{I}_n \tag{16}$$

where $\boldsymbol{I}_n \in \mathbb{R}^{n\times n}$ is a identity matrix, $\underline{m}$ and $\bar{m}$ are positive contants and defined as follows

$$\underline{m} \leq \left\| \boldsymbol{M}^{-1}(\boldsymbol{q}) \right\| \leq \bar{m} \tag{17}$$

Assumption 3. The inertial matrix $\boldsymbol{M}(\boldsymbol{q})$ is bounded for all $\boldsymbol{q}$ even in the presence of the uncertainty. In addition, the lumped disturbance $\boldsymbol{F}_d(\boldsymbol{q},\dot{\boldsymbol{q}},\ddot{\boldsymbol{q}})$ is also bounded by

$$\left\|\boldsymbol{F}_d(\boldsymbol{q},\dot{\boldsymbol{q}},\ddot{\boldsymbol{q}})\right\| < b_0 + b_1\left\|\boldsymbol{q}\right\| + b_2\left\|\dot{\boldsymbol{q}}\right\|^2 \tag{18}$$

where b_0, b_1, b_2 are unknown positive constants.

3. The proposed fractional-order sliding surface and controller design method

3.1. The proposed design methods

Before introducing the proposed method, we introduce some nonlinear functions, which are mentioned in some literature [33–34]

$$s^p(x) = \begin{cases} |x|^p \operatorname{sgn}(x), & |x| \geq \delta \\ \delta^{p-1}x, & |x| < \delta \end{cases} \tag{19}$$

where $0 < p < 1$ and $0 < \delta \leq 1$ are two positive constants, and sgn(.) is the standard signum function.

The first derivative of $s^p(x)$ with respect to x is derived as follows:

$$f^p(x) = \begin{cases} p|x|^{p-1} \operatorname{sgn}(x), & |x| \geq \delta \\ \delta^{p-1}, & |x| < \delta \end{cases} \tag{20}$$

Another nonlinear function is given by Eq. (21):

$$sig^{\mu}(x) = |x|^{\mu} \operatorname{sgn}(x) \tag{21}$$

The purpose of our design is to develop a fractional-order non-singular fixed-time terminal sliding mode control (FONFTSMC) for robot manipulators subject to parametric uncertainties and disturbances. As a result, the tracking errors asymptotically converge to the origin in a fixed time. The tracking error vectors include position and velocity given by:

$$\boldsymbol{e} = \boldsymbol{q} - \boldsymbol{q}_d,\ \dot{\boldsymbol{e}} = \dot{\boldsymbol{q}} - \dot{\boldsymbol{q}}_d,\ \ddot{\boldsymbol{e}} = \ddot{\boldsymbol{q}} - \ddot{\boldsymbol{q}}_d \tag{22}$$

where $\boldsymbol{q}_d$, $\dot{\boldsymbol{q}}_d$ are desired position and velocity, respectively.

We define some vectors

$$\boldsymbol{S}^p(\boldsymbol{e}) = \left[s^p(e_1),\ldots,s^p(e_n)\right]^T \tag{23}$$

$$\boldsymbol{F}^p(\boldsymbol{e}) = diag\left(f^p(e_1),\ldots,f^p(e_n)\right) \tag{24}$$

The proposed fractional-order nonlinear sliding surface is designed as

$$\boldsymbol{\sigma} = D^{\alpha}\dot{\boldsymbol{e}} + \boldsymbol{\Phi}_1\boldsymbol{e} + \boldsymbol{\Phi}_2\boldsymbol{S}^{p}(\boldsymbol{e}) \tag{25}$$

where $\boldsymbol{\sigma} = \left[\sigma_1, \sigma_2, \ldots, \sigma_n\right]^T \in \mathbb{R}^{1\times n}$; D is a fractional-order operator, and in this study it implies the Caputo fractional derivative; $\alpha \in \mathbb{R}$ is the fractional order, $0 < \alpha < 1$; $\boldsymbol{\Phi}_1, \boldsymbol{\Phi}_2 \in \mathbb{R}^{n\times n}$ are positive definite diagonal matrices; $0 < p < 1$. In Eq. (25), by using the fractional-order derivative in the first term, it combines the advantage of fractional order and fast terminal sliding mode control.

Taking derivative Eq. (25) with respect to time:

$$\dot{\boldsymbol{\sigma}} = D^{\alpha}\ddot{\boldsymbol{e}} + \boldsymbol{\Phi}_1\dot{\boldsymbol{e}} + \boldsymbol{\Phi}_2\boldsymbol{F}^{p}(\boldsymbol{e})\dot{\boldsymbol{e}} \tag{26}$$

To obtain a fast finite-time convergence in the sliding surface, the following fast-TSM type reaching law is adopted [14]

$$\dot{\boldsymbol{\sigma}} = -k_1\boldsymbol{\sigma} - k_2 sig^{\mu}(\boldsymbol{\sigma}) \tag{27}$$

where k_1 and k_2 are positive constants, $0 < \mu < 1$

Using two equations (24) and (25), the proposed controller is derived as follows:

$$\boldsymbol{\tau} = \boldsymbol{\tau}_0 + \boldsymbol{\tau}_1 + \boldsymbol{\tau}_2 \tag{28}$$

with, $\boldsymbol{\tau}_0 = \boldsymbol{C}_0(\boldsymbol{q}, \dot{\boldsymbol{q}})\dot{\boldsymbol{q}} + \boldsymbol{G}_0(\boldsymbol{q}) + \boldsymbol{M}_0(\boldsymbol{q})\ddot{\boldsymbol{q}}_d$ (29)

$$\boldsymbol{\tau}_1 = -D^{-\alpha}\left[\boldsymbol{M}_0 k_1\boldsymbol{\sigma} + \boldsymbol{M}_0 k_2 sig^{\mu}(\boldsymbol{\sigma}) + \boldsymbol{M}_0\left(\boldsymbol{\Phi}_1 + \boldsymbol{\Phi}_2\boldsymbol{F}^{p}(\boldsymbol{e})\right)\dot{\boldsymbol{e}}\right] \tag{30}$$

$$\boldsymbol{\tau}_2 = -\left(b_0 + b_1\left\|\dot{\boldsymbol{q}}\right\| + b_2\left\|\dot{\boldsymbol{q}}\right\|^2\right)\mathrm{sgn}(\boldsymbol{\sigma}) \tag{31}$$

3.2. Stability analysis

The stability of the system is proved by using Lyapunov function:

$$V = \frac{1}{2}\boldsymbol{\sigma}^T\boldsymbol{M}_0\boldsymbol{\sigma} \tag{32}$$

Differentiating V with respect to time, and substituting (26) into it yields

$$\dot{V} = \boldsymbol{\sigma}^T\boldsymbol{M}_0\dot{\boldsymbol{\sigma}} = \boldsymbol{\sigma}^T\boldsymbol{M}_0\left(D^{\alpha}\ddot{\boldsymbol{e}} + \boldsymbol{\Phi}_1\dot{\boldsymbol{e}} + \boldsymbol{\Phi}_2\boldsymbol{F}^{p}(\boldsymbol{e})\dot{\boldsymbol{e}}\right)$$

$$= \boldsymbol{\sigma}^T\left(D^{\alpha}\left[\boldsymbol{M}_0\left(\ddot{\boldsymbol{q}} - \ddot{\boldsymbol{q}}_d\right)\right] + \boldsymbol{M}_0\left(\boldsymbol{\Phi}_1 + \boldsymbol{\Phi}_2\boldsymbol{F}^{p}(\boldsymbol{e})\right)\dot{\boldsymbol{e}}\right) \tag{33}$$

$$= \boldsymbol{\sigma}^T \left(D^{\alpha} \left[\left(\boldsymbol{\tau} + \boldsymbol{F}_d - \boldsymbol{C}_0 \dot{\boldsymbol{q}} - \boldsymbol{G}_0 - \boldsymbol{M}_0 \ddot{\boldsymbol{q}}_d \right) \right] + \boldsymbol{M}_0 \left(\boldsymbol{\Phi}_1 + \boldsymbol{\Phi}_2 \boldsymbol{F}^p(\boldsymbol{e}) \right) \dot{\boldsymbol{e}} \right) \tag{34}$$

Substituting (28) to (31) into (34), we have

$$\dot{V} = \boldsymbol{\sigma}^T D^{\alpha} \left[\boldsymbol{F}_d - \left(b_0 + b_1 \|\dot{\boldsymbol{q}}\| + b_2 \|\dot{\boldsymbol{q}}\|^2 \right) \mathrm{sgn}(\boldsymbol{\sigma}) \right] - \boldsymbol{\sigma}^T \boldsymbol{M}_0 k_1 \boldsymbol{\sigma} - \boldsymbol{\sigma}^T \boldsymbol{M}_0 k_2 sig^{\mu}(\boldsymbol{\sigma}) \tag{35}$$

$$\dot{V} \le \|\boldsymbol{F}_d\| \|\boldsymbol{\sigma}\| - \left(b_0 + b_1 \|\dot{\boldsymbol{q}}\| + b_2 \|\dot{\boldsymbol{q}}\|^2 \right) \|\boldsymbol{\sigma}\| - \|\boldsymbol{M}_0\| \left(k_1 \|\boldsymbol{\sigma}\|^2 - k_2 \|\boldsymbol{\sigma}\|^{\mu} \right) \tag{36}$$

$$\dot{V} \le \|\boldsymbol{F}_d\| \|\boldsymbol{\sigma}\| - \left(b_0 + b_1 \|\dot{\boldsymbol{q}}\| + b_2 \|\dot{\boldsymbol{q}}\|^2 \right) \|\boldsymbol{\sigma}\| - \|\boldsymbol{M}_0\| \left(k_1 \|\boldsymbol{\sigma}\|^2 - k_2 \|\boldsymbol{\sigma}\|^{\mu} \right) \tag{37}$$

$$\dot{V} \le -\left[\rho + \|\boldsymbol{M}_0\| \left(k_1 \|\boldsymbol{\sigma}\| + k_2 \|\boldsymbol{\sigma}\|^{\mu-1} \right) \right] \|\boldsymbol{\sigma}\| \tag{38}$$

where $\rho = \left(b_0 + b_1 \|\dot{\boldsymbol{q}}\| + b_2 \|\dot{\boldsymbol{q}}\|^2 \right) - \|\boldsymbol{F}_d\| > 0$ according to Eq. (18).

$$\dot{V} \le -\left[\rho + 2\|\boldsymbol{M}_0\| \sqrt{k_1 k_2} \|\boldsymbol{\sigma}\|^{\mu/2} \right] \|\boldsymbol{\sigma}\| = -\left(\rho \|\boldsymbol{\sigma}\| + 2\|\boldsymbol{M}_0\| \sqrt{k_1 k_2} \|\boldsymbol{\sigma}\|^{1+\mu/2} \right) \tag{39}$$

$$\dot{V} \le -2\sqrt{2\rho \|\boldsymbol{M}_0\| \sqrt{k_1 k_2} \|\boldsymbol{\sigma}\|^{2+\mu/2}} = -\varphi \|\boldsymbol{\sigma}\|^{1+\mu/4} \le 0 \tag{40}$$

where $\varphi = 2\sqrt{2\rho \|\boldsymbol{M}_0\| \sqrt{k_1 k_2}}$

From Eq. (16) and (32), we have:

$$V = \frac{\|\boldsymbol{\sigma}\|^2}{\underline{m} + \bar{m}} \Rightarrow \|\boldsymbol{\sigma}\| = \sqrt{\underline{m} + \bar{m}} V^{1/2} \tag{41}$$

$$\dot{V} \le -\varphi \left(\sqrt{\underline{m} + \bar{m}} \right)^{1+\mu/4} V^{1/2+\mu/8} = -\varphi_1 V^{\beta} \tag{42}$$

where $\varphi_1 = \varphi \left(\sqrt{\underline{m} + \bar{m}} \right)^{1+\mu/4}$, $\beta = \frac{1}{2} + \frac{\mu}{8}$ (43)

Remark 2. According to Lemma 1, the global convergence of $\boldsymbol{\sigma}$ to zero in the fixed-time (t_1) is guaranteed. Based on inequalities (10), (12), (42), and (43) with $\beta = 1/2 + \mu/8$ ($\beta < 1$), $\alpha = \varphi_1$ and if $t_0 = 0$, we have:

$$t_1 = \frac{V^{1/2-\mu/8}(0)}{\varphi_1 \left(\frac{1}{2} - \frac{\mu}{8} \right)} \tag{44}$$

In addition, if the sliding surface converges to zero, the tracking errors of each joint of the manipulator will also reach zero.

4. The numerical simulation

4.1. The dynamic equations

In this section, the proposed FONTSMC is applied for trajectory tracking of two-link rigid robot manipulator [17–19], and [33]. The mass, centrifugal Coriolis and gravity matrix of the manipulator are given as follows:

$$\boldsymbol{M}(\boldsymbol{q}) = \begin{bmatrix} M_1 + 2M_2 c_2 & M_3 + M_2 c_2 \\ M_3 + M_2 c_2 & M_4 \end{bmatrix} \tag{45}$$

$$\boldsymbol{C}(\boldsymbol{q})\dot{\boldsymbol{q}} = \begin{bmatrix} -M_2 s_2 \left(\dot{q}_1^{\,2} + 2\dot{q}_1 \dot{q}_2 \right) \\ M_2 s_2 \dot{q}_2^{\,2} \end{bmatrix} \tag{46}$$

$$\boldsymbol{G}(\boldsymbol{q}) = \begin{bmatrix} G_1 c_2 + G_2 c_{12} \\ G_2 c_{12} \end{bmatrix} \tag{47}$$

where, $M_1 = (m_1 + m_2) l_1^{\,2} + m_2 l_2^{\,2} + J_1$, $M_2 = m_2 l_1 l_2$,

$M_3 = m_2 l_2^{\,2}$, $M_4 = M_3 + J_2$, $G_1 = (m_1 + m_2) l_1 g$, $G_2 = m_2 l_2 g$

$c_2 = \cos(q_2)$, $s_2 = \sin(q_2)$, $c_{12} = \cos(q_1 + q_2)$

The sampling time is chosen as 1 ms and in order to be convenient for simulation and fair to make comparisons with other methods. The robot parameters, desired trajectories, and external disturbances are the same as [17–19], [33] and are tabulated in Table 1 with SI units.

Table 1. Simulation parameters

Symbol	Description	Value
m_1	mass of the first link	0.5
m_2	mass of the second link	1.5
m_{10}	nominal mass of the first link	0.4
m_{20}	nominal mass of the second link	1.2
l_1	length of the first link	1
l_2	length of the second link	0.8
J_1	moment of inertia of the first link	5
J_2	moment of inertia of the second link	5
$[q_{d1}, q_{d2}]^{\mathrm{T}}$ (desired trajectories)	$q_{d1} = 1.25 - 1.4e^{-t} + 0.35e^{-4t}$ $q_{d2} = 1.25 + e^{-t} - 0.25e^{-4t}$	

$[\tau_{d1}, \tau_{d2}]^T$ (external disturbances)	$\tau_{d1} = 2\sin(t) + 0.5\sin(200\pi t)$ $\tau_{d1} = \cos(2t) + 0.5\sin(200\pi t)$

4.2. The methods for comparisions

The proposed method is compared with two other approaches which are the nonsingular fast terminal sliding mode control (NFTSMC) [17] and the robust fixed-time sliding mode control (RFTSMC) [33]. To easily follow the simulation results, the two above control methods are summarized below. The main equations of NFTSMC [17] are

$$\boldsymbol{\sigma} = \boldsymbol{e} + sig^{\boldsymbol{\Gamma}_1}(\boldsymbol{e}) + sig^{\boldsymbol{\Gamma}_2}(\dot{\boldsymbol{e}}) \tag{48}$$

$$\boldsymbol{\tau} = -\boldsymbol{M}_0(\boldsymbol{q})\left[K_2\boldsymbol{\sigma} + (\rho + K_1)\frac{\boldsymbol{\sigma}}{\|\boldsymbol{\sigma}\|} + \boldsymbol{F}_2 + \boldsymbol{\Gamma}_2^{-1}\left(\boldsymbol{I}_2 + \boldsymbol{\Gamma}_1 diag(|\boldsymbol{e}|^{\boldsymbol{\Gamma}_1 - \boldsymbol{I}_2})\right) sig^{2\boldsymbol{I}_2 - \boldsymbol{\Gamma}_2}(\dot{\boldsymbol{e}}) \right] \tag{49}$$

with $\boldsymbol{\rho} = \left\| M_0^{-1} \right\| \left(b_0 + b_1 \|\boldsymbol{q}\| + b_2 \|\dot{\boldsymbol{q}}\|^2 \right)$

$$\boldsymbol{F}_2 = -\boldsymbol{M}_0(\boldsymbol{q})^{-1}\left(\boldsymbol{C}_0(\boldsymbol{q}, \dot{\boldsymbol{q}})\dot{\boldsymbol{q}} + \boldsymbol{G}_0(\boldsymbol{q})\right) - \ddot{\boldsymbol{q}}_d \tag{50}$$

where K_1, K_2 are positive constants, $\boldsymbol{\Gamma}_1, \boldsymbol{\Gamma}_2 \in \mathbb{R}^{n \times n}$ are the constant matrices. $\boldsymbol{M}_0$, $\boldsymbol{C}_0$, $\boldsymbol{G}_0$, and b_0, b_1, b_2 are defined in section 2.2

And the RFTSMC [33] has the following control laws:

$$\boldsymbol{\sigma} = \dot{\boldsymbol{e}} + \boldsymbol{K}_1 \boldsymbol{S}^p(\boldsymbol{e}) + \boldsymbol{K}_2 \boldsymbol{sig}^r(\boldsymbol{e}) \tag{51}$$

$$\boldsymbol{\tau} = \boldsymbol{M}_0(\boldsymbol{q})\ddot{\boldsymbol{q}}_d + \boldsymbol{C}_0(\boldsymbol{q}, \dot{\boldsymbol{q}})\dot{\boldsymbol{q}} + \boldsymbol{G}_0(\boldsymbol{q}) - \boldsymbol{K}_0 \boldsymbol{sig}^{\eta}(\boldsymbol{\sigma}) - \boldsymbol{M}_0\left(\boldsymbol{K}_1 \boldsymbol{F}^p(\boldsymbol{e}) + r\boldsymbol{K}_2 diag(|\boldsymbol{e}|^{r-1})\right)\dot{\boldsymbol{e}} - \frac{\boldsymbol{\sigma}}{\|\boldsymbol{\sigma}\|}u \tag{52}$$

with $u = \frac{1}{1-\gamma}\left(u_0 + b_0 + b_2 \|\dot{\boldsymbol{q}}\|^2 + \gamma \|\boldsymbol{\tau}_0 + \boldsymbol{\tau}_1\|\right)$, (53)

$$\gamma = \frac{\bar{m} - \underline{m}}{\bar{m} + \underline{m}} < 1 \ \left(\underline{m} \le \left\|\boldsymbol{M}^{-1}(\boldsymbol{q})\right\| \le \bar{m}\right) \tag{54}$$

where $\boldsymbol{K}_0, \boldsymbol{K}_1, \boldsymbol{K}_2 \in \mathbb{R}^{n \times n}$ are positive diagonal matrices, $0 < p < 1$, $r > 1$, $\eta > 1$, $u_0 > 0$, b_0 and b_2 are defined in section 2.2.

Table 2. Control parameters of two comparision methods

Methods	Parameters

NFTSMC	$\boldsymbol{\Gamma}_1 = diag\left([2,2]\right), \boldsymbol{\Gamma}_2 = diag\left([7/5,7/5]\right)$
	$K_1 = 2, K_2 = 1,\ b_0 = 12,\ b_1 = 2.2,\ b_2 = 2.8$
RFTSMC	$\boldsymbol{K}_0 = \boldsymbol{K}_1 = \boldsymbol{K}_2 = diag\left([2,2]\right),\ p = 0.5,\ r = 1.2\ ,$
	$\eta = 1.5,\ u_0 = 1,\ b_0 = 12,\ b_2 = 2.8$

For a fair comparison, the control parameters of the NFTSMC and RFTSMC are chosen as [17] and [33], respectively. The parameters of two methods are summarized in Table 2.

4.3.Simulation results

For simulation, all robot parameters are chosen as Table 1. The upper bounds of the uncertainty are given the same in all methods ($b_0 = 12,\ b_1 = 2.2,\ b_2 = 2.8$) as Table 2.

From Eq. (17), (45) and Table 1, we also calculate the lower and upper bounds of the inverse inertial matrix, $\underline{m} = 0.09$ and $\overline{m} = 0.2$, respectively.

Other control parameters are chosen as follows:

$\boldsymbol{\Phi}_1 = diag\left([20,20]\right),\ \boldsymbol{\Phi}_2 = diag\left([1.5,1.5]\right),\ k_1 = k_2 = 2,\ \mu = 0.9,\ \alpha = 0.1,\ p = 0.5$

The initial conditions of all joints are assigned as:

$\left[\boldsymbol{q}^T(0) \quad \dot{\boldsymbol{q}}^T(0)\right]^T = [1 \quad 1.5 \quad 0 \quad 0]^T$

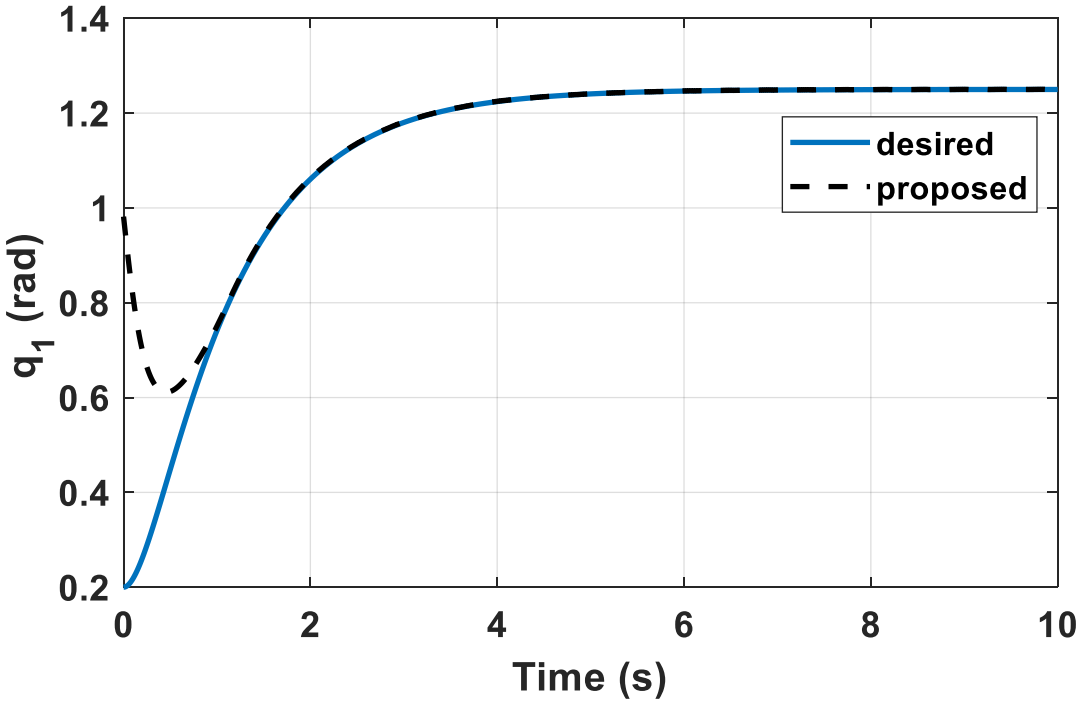


Figure 1. The position tracking response of the first joint

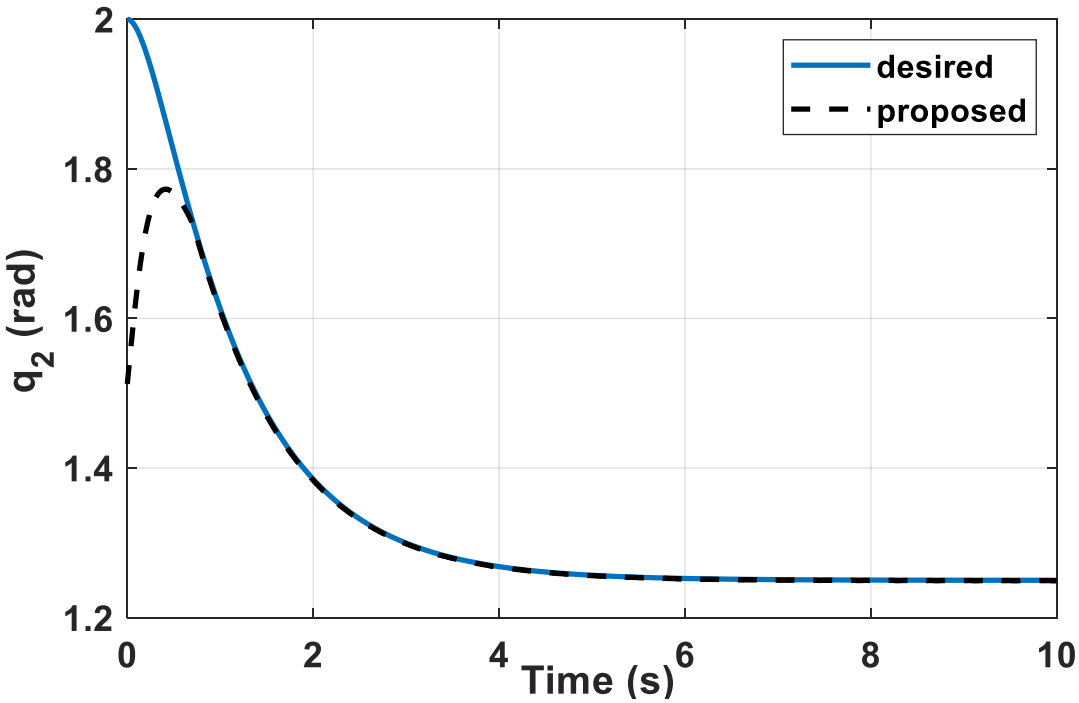
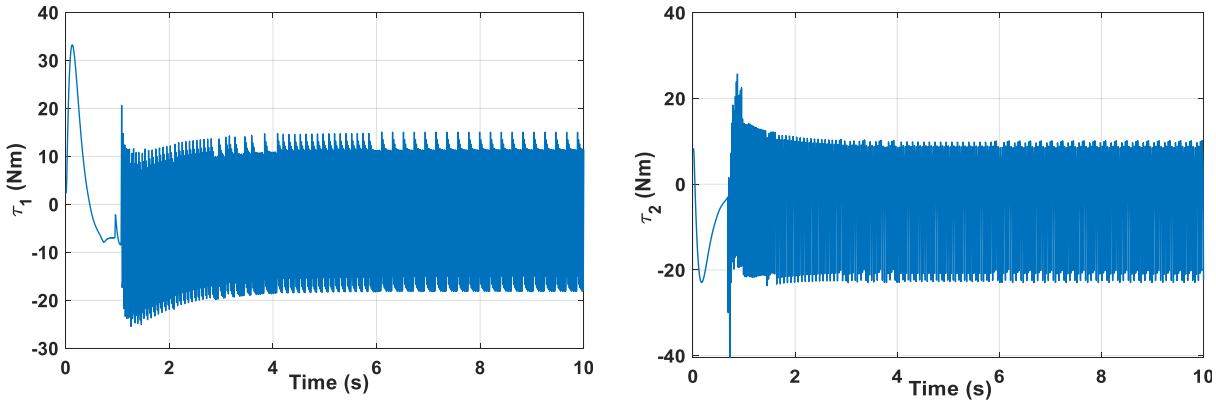


Figure 2. The position tracking response of the second joint

Figure 1 and 2 show the position tracking response of the proposed method. It can be seen that the joint responses track the desired trajectories precisely and quickly. However, Figure 3 (a) and (b) indicate that the control inputs of both joints have chattering phenomenon due to the discontinuous part in the control law. Therefore, remark 3 helps to deal with this problem.



(a) (b)

Figure 3. The control inputs of the first (a) and second (b) joints

Remark 3. In order to eliminate the chattering phenomenon, the discontinuous part in Eq. (31) of the proposed control law is replaced by the nonlinear function (19)

$$\boldsymbol{\tau}_2 = \begin{cases} -\left(b_0 + b_1 \|\dot{\boldsymbol{q}}\| + b_2 \|\dot{\boldsymbol{q}}\|^2\right)|\sigma|^p \operatorname{sgn}(\sigma), \left(|\sigma| \geq \delta\right) \\ -\left(b_0 + b_1 \|\dot{\boldsymbol{q}}\| + b_2 \|\dot{\boldsymbol{q}}\|^2\right)\delta^{p-1}\sigma, \qquad \left(|\sigma| \geq \delta\right) \end{cases} \tag{55}$$

where δ is a small value, and in this work $\delta = 0.01$

Figures 4 and 5 show the position tracking of two joints when replacing Eq. (55) into the proposed control law. In addition, we also compare the responses with other mentioned methods in section 4.2. From the figures, we can see that all controllers ensure the tracking problem of the robot. After the errors in transient response due to initial conditions, the position tracking errors converge to zero over time. However, the proposed method still gives the fastest convergence compared to other methods.

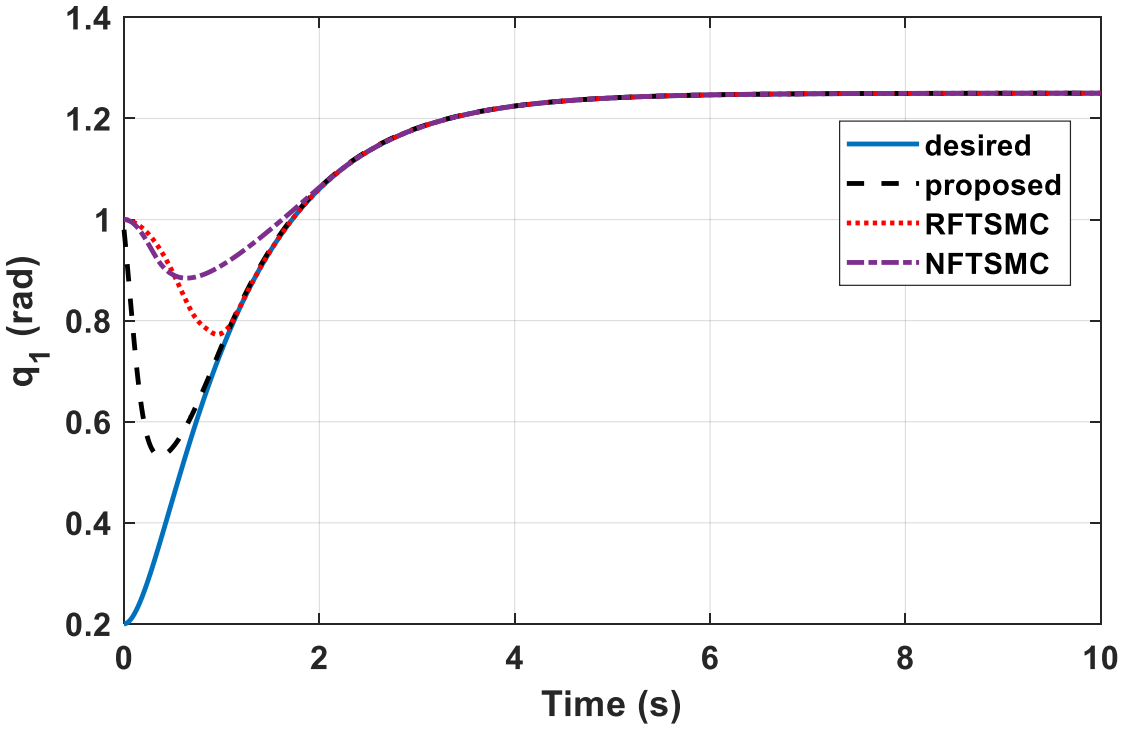


Figure 4. Position tracking responses of the first joint of all methods

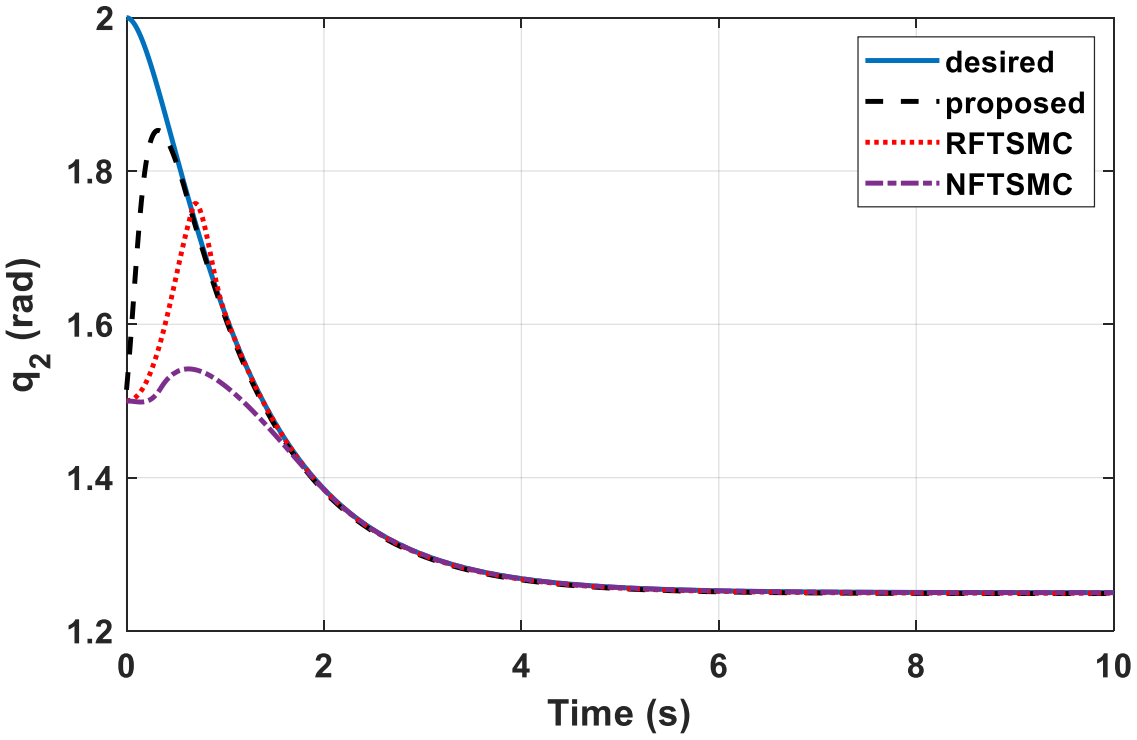


Figure 5. Position tracking responses of the second joint of all methods

Figures 6 and 7 illustrate the control torques of all methods of the first and second joints, respectively. It is obvious that the input signals are continuous and chattering-free for all methods. In addition, at the steady state, all methods have almost the same values of the torque, especially the proposed method and RFTSMC have identical values of the requested torque at this state. However, in the transient response, there are differences among those methods. Therefore, for the quantitative comparison, two well-known criteria, which are integral absolute error (IAE) and integral of time-weighted absolute error (ITAE), are adopted for evaluating the steady state tracking errors. The control input effort (CIE) is also suggested to compare the control torques of all methods. The calculations of these indices are given by the following equations, respectively.

$$\mathrm{IAE} = \int_0^{\tau} |e(t)|\,dt \approx \sum_{k=1}^{N} |e(k)| \tag{56}$$

$$\mathrm{ITAE} = \int_0^{\tau} t\,|e(t)|\,dt \approx \sum_{k=1}^{N} t(k)\,|e(k)| \tag{57}$$

$$\mathrm{CIE} = \sqrt{\frac{1}{N}\sum_{k=1}^{N} |u(k)|^2} \tag{58}$$

where τ is simulation time; N is the total sample in the running time; $t(k)$, $e(k)$, and $u(k)$ are the values of time, error, and control input at the k^{th} sampling instant, respectively.

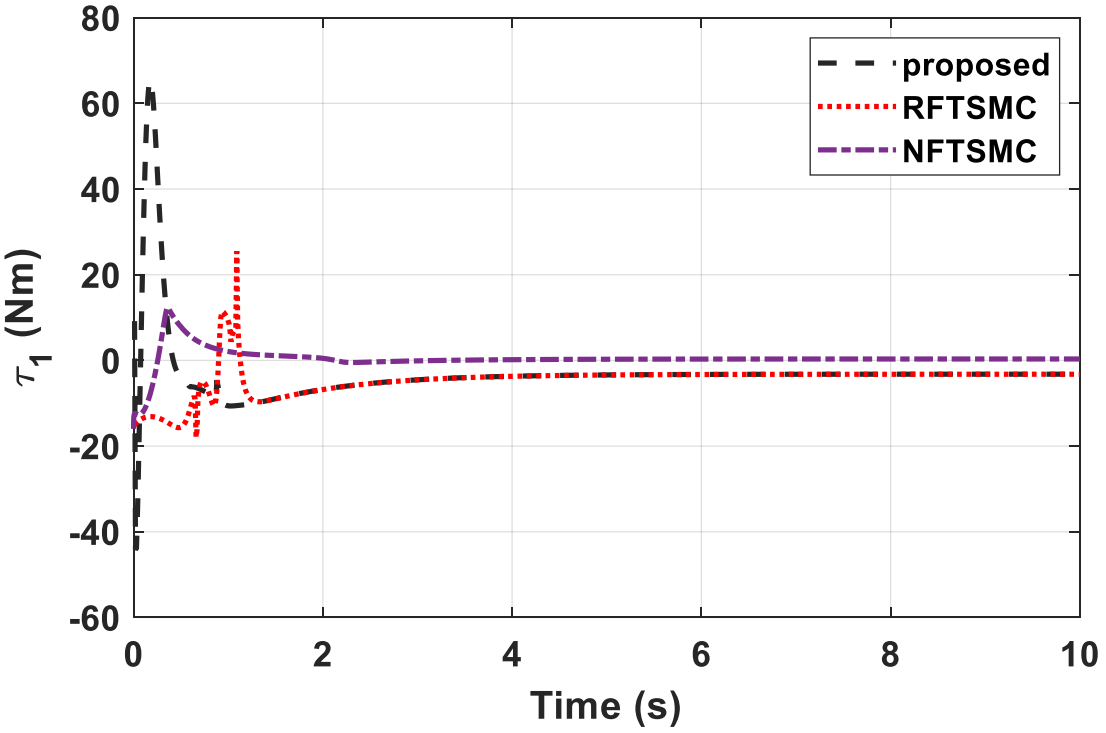


Figure 6. Control torques of the first joint

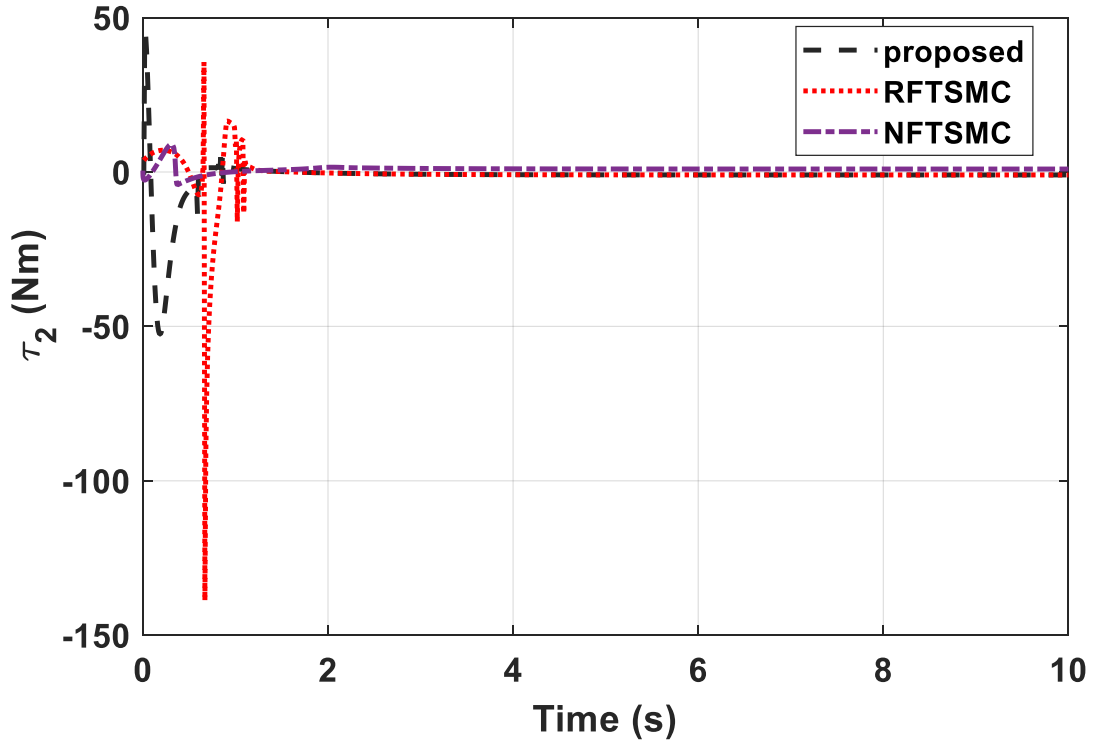


Figure 7. Control torques of the second joint

From Table 3, the proposed method obtains the minimal IAE and ITAE compared to NFTSMC and RFTSMC. Although the CIE values of the FTSMC are higher than those of other methods, there are no excessive control gains in the proposed method. Therefore, it can be concluded that the proposed method achieves better tracking performance compared to the NFTSMC and RFTSMC.

Table 3. Perfromance indices of all methods

Controllers	Joints	IAE	ITAE	CIE
Proposed	1	0.197	0.047	3.456
(FTSMC)	2	0.103	0.092	1.599
NFTSMC	1	0.507	0.174	0.241
	2	0.318	0.108	0.145
RFTSMC	1	0.441	0.152	0.579
	2	0.214	0.093	0.739

To evaluate the effect of the initial conditions on the fixed-time convergence, three different initial conditions of two joints are considered: (0.5, 1.0), (1.0, 0.5), and (1.2, 1.2). Figures 8 and 9 show the responses of the two joints under these conditions. It can be observed that the settling times in all cases are nearly identical. Assuming a settling time of approximately 1 (s), Table 4 summarizes the angular positions (in radians) of both joints at t = 1 s. The results clearly indicate that the joint positions converge to consistent values regardless of the initial conditions, thereby confirming the fixed-time convergence property of the proposed controller.

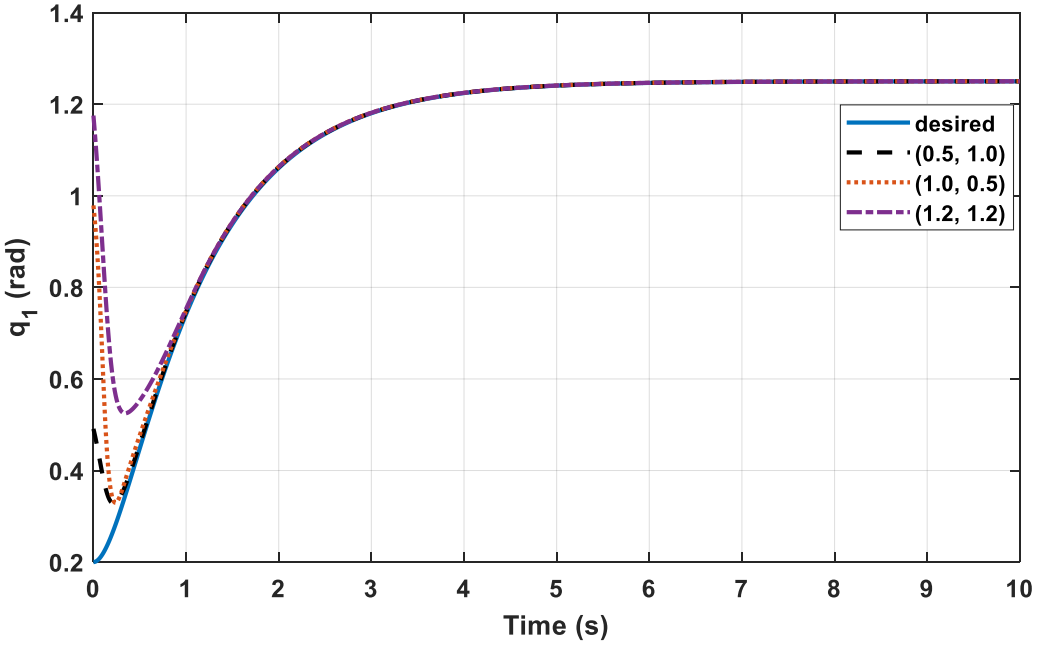


Figure 8. The responses of the first joint with three different intial conditions

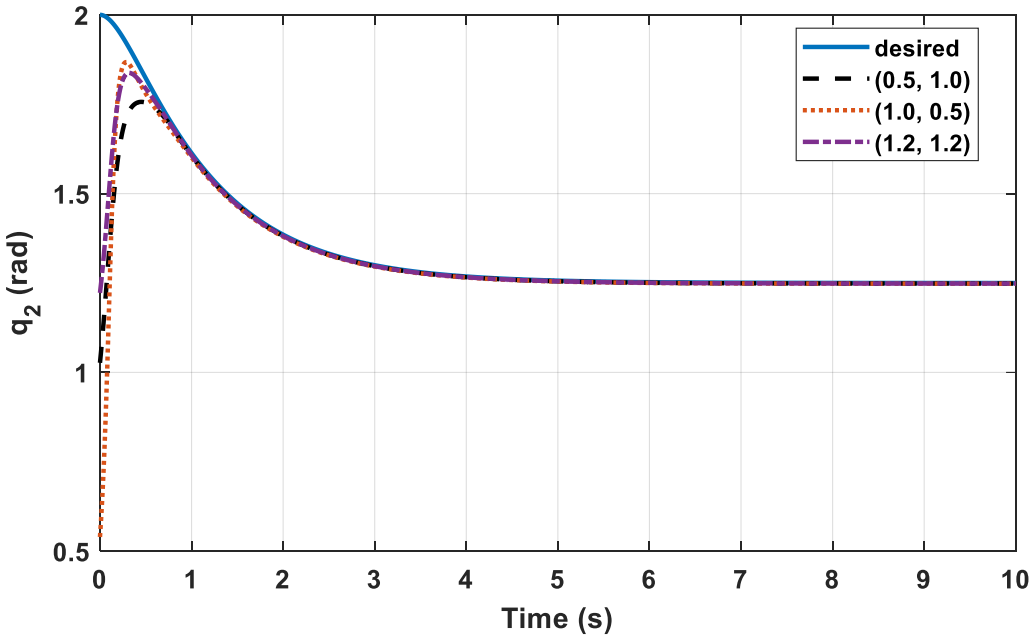


Figure 9. The responses of the second joint with three different intial conditions

Table 4. The joint positions at the settling time 1 (s) with different initial conditions

Initial conditions (rad)	Joints	(q_1, q_2) (rad)	The settling time (s)
(0.5, 1.0)	1	0.7467	1
	2	0.1606	
(1.0, 0.5)	1	0.7414	
	2	1.6050	
(1.2, 1.2)	1	0.7485	
	2	1.6070	

5. Conclusion

In this paper, a novel sliding surface using fractional calculus and non-singular fast terminal sliding mode control has been proposed for trajectory tracking control of uncertain robot manipulators with bounded disturbances. The simulation study in the 2-dof robot manipulators illustrates the effectiveness of the proposed method. The results are also compared with the NFTSMC and RFTSMC methods. Due to utilizing the fractional-order sliding surface, the tracking performances are faster and more precise than integer-order ones. However, it also costs more control efforts than other methods, but the control gains are still in the appropriate range. Future research will focus on a combination of fractional order and robust/adaptive control for fixed-time and predefined-time SMC of uncertain robot manipulators subject to constraints of disturbances and actuators.

Author Contributions

Vo Lam Chuong: literature review, formula derivation, software, and writing– original draft.

Ha Le Nhu Ngoc Thanh: conceptualization, software, review and editing the manuscript.

Truong Nguyen Luan Vu: supervision, methodology, writing– review and approve the manuscript

Funding

This research is funded by Ministry of Education and Training under grant number B2024-SPK-07. The authors acknowledge HCMC University of Technology and Engineering for supporting this study.

Data availability

The datasets used and/or analysed during the current study are available from the corresponding author on reasonable request.

Declarations

Competing interests

The authors declare no competing interests.

References

[1] Purwar, S., Kar, I.N, & Jha, A.N. Adaptive output feedback tracking control of robot manipulators using position measurements only. *Expert Syst. Appl.* **34**(4), 2789–2798 (2008).

[2] Gorji, S., & Yazdanpanah, M.J. A novel robust adaptive trajectory tracking in robot manipulators. *J. Comput. Robot*. **10**(2), 1–11 (2017).

[3] Li, D., Yuantao, Y., Zhai, D.H, Huang, T., & Xia, Y. Robust Model Predictive Tracking Control for Robot Manipulators with Disturbances. *IEEE Trans. Ind. Electron.* **68**(5), 4288–4297 (2021).

[4] Hu, Q., Xu, L., & Zhang, A. Adaptive backstepping trajectory tracking control of robot manipulator. *J. Franklin Inst*. **349**(3), 1087–1105 (2012).

[5] Yang, Z.J, Fukushima, Y., & Qin, P. Decentralized adaptive robust control of robot manipulators using disturbance observers. *IEEE Trans. Control Syst. Technol.* **20**(5), 1357–1367 (2012).

[6] Wai, R.J, & Muthusamy, R. Design of fuzzy-neural-network-inherited backstepping control for robot manipulator including actuator dynamics. *IEEE Trans. Fuzzy Syst.* **22**(4), 709–722 (2014).

[7] Liu, H., & Zhang, T. Neural network-based robust finite-time control for robotic manipulators considering actuator dynamics. *Robot. Comput. Integr. Manuf.* **29**(2), 301–308 (2013).

[8] Slotine, J.J, & Sastry, S.S. Tracking control of nonlinear systems using sliding surfaces with application to robot manipulators. *Internat. J. Control* **38**(2), 465–492 (1983).

[9] Soltanpour, M.R., Otadolajam, P., & Khooban, M.H. Robust control strategy for electrically driven robot manipulators: adaptive fuzzy sliding mode. *IET Sci. Meas. Technol.* **9**(3), 322–334 (2015).

[10] Baek, J., Jin, M., & Han, S. A new adaptive sliding mode control scheme for application to robot manipulators. *IEEE Trans. Ind. Electron.* **63**(6), 3628–3637 (2016).

[11] Man, Z., Palaniswami, M., & Wu, H.R. A robust MIMO terminal sliding mode control scheme for rigid robotic manipulators. *IEEE Trans. Autom. Control* **39**(12), 2464–2469 (1994).

[12] Tang, Y. Terminal sliding mode control for rigid robots. *Automatica*, **34**(1), 51–56 (1998).

[13] Feng, Y., Yu, X., & Man, Z. Non-singular terminal sliding mode control of rigid manipulators. *Automatica*, **38**(12), 2159 – 2167 (2002).
[14] Yu, S., Yu, X., Shirinzadeh, B., & Man, Z. Continuous finite-time control for robotic manipulators with terminal sliding mode. *Automatica*, **41**(11), 1957–1964 (2005).
[15] Galicki, M. Finite-time control of robotic manipulators. *Automatica*, **51**, 49–54 (2015).
[16] Jin, M., Lee, J., Chang, P., & Choi, C. Practical nonsingular terminal sliding mode control of robot manipulators for high-accuracy tracking control. *IEEE Trans. Ind. Electron*., **59**(9), 3593–3601 (2009).
[17] Yang, L., & Yang, J.Y. Nonsingular fast terminal sliding-mode control for nonlinear dynamical systems. *Int. J. Robust Nonlinear Control*, **21**(16), 1865–1879 (2011).
[18] Boukattaya, M., Mezghani, N., Damak, T. Adaptive nonsingular fast terminal sliding-mode control for the tracking problem of uncertain dynamical systems. *ISA Trans.*, **77**, 1–19 (2018).
[19] Shanchao, Y., Junyong, Z. Adaptive second-order fast nonsingular terminal sliding mode control for robotic manipulators. *ISA Trans.*, **90**, 41–51 (2019).
[20] Tian, Y., Cai, Y., & Deng, Y. A fast nonsingular terminal sliding mode control method for nonlinear systems with fixed-time stability guarantees. *IEEE Access* **8**, 60444–60454 (2020).
[21] Podlubny, I. Fractional-Order Systems and $PI^{\lambda}D^{\mu}$-Controllers. *IEEE Trans. Autom. Control*, **44**, 208–214 (1999).
[22] Monje, C.A., Chen, Y., Vinagre, B.M., Xue, D., & Feliu-Batlle, V. *Fractional-Order Systems and Controls, Fundamentals and Applications* (Springer, London, UK, 2010).
[23] Beschi, M., Padula, F., & Visioli, A. Fractional robust PID control of a solar furnace. *Control Eng. Pract.*, **60**, 190–199 (2016).
[24] Sánchez, H.S., Padula, F., Visioli, A., & Vilanova, R. Tuning rules for robust FOPID controllers based on multi-objective optimization with FOPDT models. *ISA Trans.*, **66**, 344–361 (2017).
[25] Mousavi, Y., Zarei, A., & Jahromi, Z.S. Robust adaptive fractional-order nonsingular terminal sliding mode stabilization of three-axis gimbal platforms. *ISA Trans.*, **123**, 98–109 (2022).
[26] Dadras, S., Momeni, H.R. Fractional terminal sliding mode control design for a class of dynamical systems with uncertainty. *Commun. Nonlinear Sci. Numer. Simulat.*, **17**, 367–377 (2012).
[27] Wang, J., Zhou, Y., Bao, Y., Hynn, H.K, Min, C.L. Trajectory Tracking Control Using Fractional-Order Terminal Sliding Mode Control with Sliding Perturbation Observer for a 7-DOF Robot Manipulator. *IEEE/ASME Trans. Mechatron.*, **25**(4), 1886–1893 (2020).
[28] Nojavanzadeh, D., & Badamchizadeh, M. Adaptive fractional-order non-singular fast terminal sliding mode control for robot manipulators. *IET Control Theory Appl*. **10**(13), 1565–1572 (2016).
[29] Zhang, X., & Quan, Y. Adaptive fractional-order non-singular fast terminal sliding mode control based on fixed time disturbance observer for manipulators. *IEEE Access* **10**, 76504 –76511 (2022).
[30] Wu, X., Huang, Y. Adaptive fractional-order non-singular terminal sliding mode control based on fuzzy wavelet neural networks for omnidirectional mobile robot manipulator. *ISA Trans.* **121**, 258–267 (2022).
[31] Li, Y., Chen, YQ., & Podlubny, I. Mittag-Leffler stability of fractional order nonlinear dynamic systems *Automatica*, **45**, 1965–1969 (2009).
[32] Spong, M.W., Hutchinson, S., Vidyasagar, M. *Robot Modeling and Control* (John Wiley & Sons, Hoboken, NJ, 2006).
[33] Su, Y., Zheng, C., Mercorelli, P. Robust approximate fixed-time tracking control for uncertain robot manipulators. *Mech. Syst. Signal Pr*. **135**, 106379 (2020).
[34] Zheng, C., Su, Y., Mercorelli, P. A simple nonlinear PD control for faster and high-precision positioning of servomechanisms with actuator saturation. *Mech. Syst. Signal Pr.* **121**, 215–226 (2019).